



Molecular Crystals and Liquid Crystals Incorporating Nonlinear Optics

Publication details, including instructions for authors and
subscription information:

<http://www.tandfonline.com/loi/gmcl17>

Isotropic-Liquid Crystal Phase Equilibrium in Semiflexible Polymer Solutions: Application of Scaled Particle Theory

T. Sato^a & A. Teramoto^a

^a Department of Macromolecular Science, Osaka University,
Toyonaka, Osaka, 560, Japan

Version of record first published: 04 Oct 2006.

To cite this article: T. Sato & A. Teramoto (1990): Isotropic-Liquid Crystal Phase Equilibrium in Semiflexible Polymer Solutions: Application of Scaled Particle Theory, *Molecular Crystals and Liquid Crystals Incorporating Nonlinear Optics*, 178:1, 143-155

To link to this article: <http://dx.doi.org/10.1080/00268949008042715>

PLEASE SCROLL DOWN FOR ARTICLE

Full terms and conditions of use: <http://www.tandfonline.com/page/terms-and-conditions>

This article may be used for research, teaching, and private study purposes. Any substantial or systematic reproduction, redistribution, reselling, loan, sub-licensing, systematic supply, or distribution in any form to anyone is expressly forbidden.

The publisher does not give any warranty express or implied or make any representation that the contents will be complete or accurate or up to date. The accuracy of any instructions, formulae, and drug doses should be independently verified with primary sources. The publisher shall not be liable for any loss, actions, claims, proceedings, demand, or costs or damages whatsoever or howsoever caused arising directly or indirectly in connection with or arising out of the use of this material.

Isotropic-Liquid Crystal Phase Equilibrium in Semiflexible Polymer Solutions: Application of Scaled Particle Theory

T. SATO and A. TERAMOTO

Department of Macromolecular Science, Osaka University, Toyonaka, Osaka 560, Japan

(Received June 1, 1989; in final form August 25, 1989)

The scaled particle theory of Cotter for straight spherocylinders was extended to semiflexible polymer solutions following Khokhlov and Semenov's procedure to calculate the isotropic-liquid crystal phase boundary concentrations and osmotic pressure of the solution, with the diameter d and persistence length q of the polymer as parameters. The calculated phase boundary concentrations and osmotic pressure were compared favorably with experimental data for aqueous schizophyllan (a triple helical polysaccharide) and poly(hexyl isocyanate) in toluene and dichloromethane when use was made of the experimental q values and the d values rather close to those obtained from the partial specific volume of the polymer. Thus the thermodynamic behavior of the systems investigated was explained essentially in terms of the hard-core potential.

INTRODUCTION

Moderately concentrated solutions of stiff-chain polymers in good solvent can form a liquid crystal (nematic or cholesteric) phase. Since stiff-chain polymers interact with each other by a repulsive force in a good solvent, it follows that the liquid crystal formation in such a system is mainly due to the repulsive interaction among stiff-chain polymer molecules. This is in contrast to thermotropic liquid crystals of low molecular weight mesogens, where, as is well-known, the van der Waals attractive interaction plays an important role.^{1,2}

Thermodynamic properties of concentrated solutions of stiff-chain polymers have been studied for a long time by many workers.^{3–11} Among them were Kubo and Ogino⁵ who measured osmotic pressure of poly(γ -benzyl-L-glutamate) (PBLG) solutions and showed that their data could be interpreted well by the scaled particle (SP) theory of Cotter¹² for systems of hard spherocylinders. Later, Brian *et al.*⁷ reached a similar conclusion with their data for aqueous DNA solutions. However, Kubo and Ogino pointed out that their experimental isotropic-liquid crystal phase boundary concentrations did not agree with the prediction by the SP theory. This disagreement was attributed to the flexibility of PBLG molecule.

On the other hand, Itou and Teramoto¹⁰ demonstrated that Khokhlov and Se-

menov's (KS) theory¹³ for semiflexible polymer solutions could predict accurately the isotropic-liquid crystal phase boundary concentrations experimentally obtained for aqueous solutions of schizophyllan (a triple helical polysaccharide) and toluene solutions of poly(hexyl isocyanate) (PHIC). However, the KS theory is an extension of the Onsager theory¹⁴ for rodlike polymer solutions and uses the second virial approximation at formulating the free energy function. Thus it may be less accurate than the SP theory which considers the higher virial terms as well. In fact, Itou *et al.*¹¹ recently showed that the third and higher virial terms in osmotic pressure (or solvent chemical potential) could not be neglected for toluene and dichloromethane (DCM) solutions of PHIC even at concentrations much lower than the phase boundary concentration.

In order to find a theoretical formulation of semiflexible polymer solutions valid at higher concentrations, we extended the scaled particle theory of Cotter¹² to wormlike spherocylinders following essentially the same procedure as that of Khokhlov and Semenov.¹³ This paper presents the basic equations of the theory and the isotropic-nematic phase boundary concentrations calculated therefrom. This extended scaled particle (ESP) theory is tested with experimental data for the osmotic pressure and the isotropic-liquid crystal phase boundary concentrations of aqueous schizophyllan^{8,9} and toluene and DCM solutions of PHIC.^{10,11}

THEORY

The scaled particle theory was originally proposed for hard sphere fluids by Reiss *et al.*¹⁵ Several investigators^{12,16-18} attempted to extend this theory to hard cylinder or spherocylinder systems. Among them, Cotter¹² modified her own theory¹⁸ and obtained an expression for the Helmholtz free energy ΔF of a system consisting of n hard spherocylinders which have the diameter d and the cylinder length L and interact each other only by the hard-core potential. As a function of the number density c' of spherocylinders, ΔF is written as

$$\begin{aligned} \Delta F/(nk_B T) = & \ln[c'/(1 - v_0 c')] - 1 + \sigma + 3v_0 c'/(1 - v_0 c') \\ & + bc' \rho [1 - (1 - g)v_0 c'/3]/(1 - v_0 c')^2 \\ & + (v_0 c')^2 (4 + g - g^2/2)/[3(1 - v_0 c')^2] \end{aligned} \quad (1)$$

Here

$$v_0 = \pi(d/2)^2 L + (4\pi/3)(d/2)^3 \quad (2)$$

$$b = (\pi/4)dL^2 \quad (3)$$

$$g = (4\pi/3)(d/2)^3/v_0 \quad (4)$$

and σ and ρ are defined by

$$\sigma = \int f(\Omega) [\ln 4\pi f(\Omega)] d\Omega \quad (5)$$

$$\rho = (4/\pi) \iint |\sin \gamma(\Omega, \Omega')| f(\Omega) f(\Omega') d\Omega d\Omega' \quad (6)$$

where $f(\Omega)$ is the orientational distribution function and $\gamma(\Omega, \Omega')$ is the angle between two cylinders oriented at Ω and Ω' ; $nk_B\sigma$ represents the orientational entropy loss on going from the isotropic state to liquid crystal state, while ρ expresses the reduction of the excluded volume due to the orientation.

This free energy function of the Cotter theory agrees with Onsager's ΔF for spherocylinder gases:¹⁴

$$\Delta F/(nk_B T) = \ln c' - 1 + \sigma + (b\rho + 4v_0)c' \quad (7)$$

up to the second virial term. (The third virial coefficient B_3 of the Cotter theory is compared with Straley's numerical calculation¹⁹ of B_3 in the Appendix.) On the other hand, at $L = 0$, Equation 1 reduces to the expression of Reiss *et al.*¹⁵ for hard spheres. Further this Cotter's theory yields the equation of state which is in good agreement with data of computer simulation for hard spherocylinder fluids.¹² Although Equation 1 was proposed for one component system of spherocylinders, it can be applied to an athermal system of hard spherocylinders and small molecular solvent, if ΔF is considered as the excess free energy over that of the pure solvent.

Now we consider an athermal solution of wormlike spherocylinders with the cylinder contour length L and the diameter d ; the spherocylinders interact each other only by the hard-core potential and the cylinder axis follows the wormlike chain statistics. We derive an expression for the Helmholtz free energy of this system by incorporating the effect of flexibility into Equation 1 following the procedure of Khokhlov and Semenov¹³ who used Equation 7 for the same purpose. The following two contributions to the free energy need separate consideration.

The orientational entropy contribution

The orientation of the wormlike cylinders in the system is specified by the orientational distribution function $f(\Omega)$ of the unit vectors tangential to the cylinder axis, and the formation of liquid crystal phase in this system produces the entropy loss due to the orientation of the tangent vectors. This entropy loss, which includes the conformational entropy loss of the chain as well as the orientational entropy loss of the whole chain, was calculated by Khokhlov and Semenov.¹³ By use of the Onsager trial function for $f(\Omega)$, their entropy loss $nk_B\sigma_{KS}$ is written as

$$nk_B\sigma_{KS} = nk_B[N(\alpha - 1)/2 + \ln(\alpha/4)] \quad (\alpha N \gg 1) \quad (8a)$$

$$= nk_B[\ln \alpha - 1 + N(\alpha - 1)/3] \quad (\alpha N \ll 1) \quad (8b)$$

for large and small Kuhn's statistical segment number N . Here α is the orientation parameter contained in the Onsager trial function. For the system of the wormlike chain, the term σ in Equation 1 is replaced by σ_{KS} .

The excluded volume contribution

In the right hand side of Equation 1, the terms except σ were derived from the intermolecular excluded volume of the straight spherocylinder.^{12,18} Thus, if the expression of the excluded volume b_{wsc} of wormlike spherocylinder was known, ΔF for the wormlike chain system could be calculated. However, unfortunately, b_{wsc} is not formulated exactly. (Although Yamakawa and Stockmayer²⁰ calculated the excluded volume of the wormlike beads model using the double-contact approximation, their results did not reduce to the excluded volume of the cylinder model in the rod limit. Thus their expression is not adequate to our purpose.) Here we approximate b_{wsc} by the excluded volume of the straight spherocylinder and use Equation 1 as it is for wormlike spherocylinders excepting that σ is replaced by σ_{KS} , although this approximation may become worse for larger N . In Equation 1, ρ is defined by Equation 6, where $f(\Omega)$ and $\gamma(\Omega, \Omega')$ should be regarded as the orientational distribution function of the tangent vectors of the wormlike chain and the angle between two tangent vectors belonging to different chains, respectively. Using the Onsager trial function for $f(\Omega)$, ρ is written as¹⁴

$$\rho = [4/(\pi\alpha)^{1/2}][1 - 15/16\alpha + 105/512\alpha^2 + 315/8192\alpha^3 + o(\alpha^{-4})] \quad (9)$$

The osmotic pressure Π of the solution and the chemical potential μ of the solute are derived from Equation 1 with σ_{KS} instead of σ as

$$\begin{aligned} \Pi/k_B T = & c' \{ 1 + v_0 c' + b c' \rho [1 + (1/3) v_0 c' (1 + 2g)] \\ & + (2/3) (v_0 c')^2 (1 + g - g^2/2) \} / (1 - v_0 c')^3 \end{aligned} \quad (10)$$

TABLE I

Phase boundary concentrations $v_0 c'_i$ and $v_0 c'_a$ calculated from the extended scaled particle theory. X , N , and v_0 are the axial ratio $[(L + d)/d]$, the number of Kuhn's segments, and the molecular volume of the wormlike spherocylinder, respectively.

		N					
	X	0	1.5	2	3	4	5
$v_0 c'_i$	10	0.250	0.543	0.587	0.646	0.685	0.713
	20	0.142	0.403	0.451	0.519	0.566	0.601
	30	0.100	0.324	0.372	0.442	0.491	0.529
	40	0.0768	0.273	0.318	0.386	0.436	0.475
	50	0.0624	0.236	0.278	0.344	0.394	0.433
	60	0.0526	0.208	0.248	0.311	0.360	0.399
	80	0.0400	0.168	0.204	0.262	0.308	0.345
	100	0.0323	0.142	0.173	0.226	0.269	0.303
	200	0.0164	0.0790	0.0993	0.136	0.167	0.195
	300	0.0100	0.0549	0.0697	0.0970	0.122	0.144
	400	0.0083	0.0420	0.0537	0.0756	0.0958	0.115
	500	0.0067	0.0341	0.0437	0.0619	0.0790	0.0950

and

$$\begin{aligned} \mu/k_B T = & \ln [c'/(1 - v_0 c')] + \sigma_{KS} + 6v_0 c'/(1 - v_0 c') \\ & + 2bc' \rho (1 + g v_0 c'/2)/(1 - v_0 c')^2 \\ & + (v_0 c')^2 (4 + g - g^2/2)/(1 - v_0 c')^2 + v_0 \Pi/k_B T \end{aligned} \tag{11}$$

respectively. In the isotropic state, $\sigma_{KS} = \sigma = 0$ and $\rho = 1$, and Π and μ given by Equations 10 and 11 are identical to Cotter's expressions, while in the liquid crystal state, they differ from the Cotter's owing to the differences between σ_{KS} and σ . The isotropic-nematic phase boundary concentrations can be calculated from the free energy minimization condition with respect to the degree of orientation:

$$\partial \Delta F / \partial \alpha = 0 \tag{12}$$

for ΔF given by Equation 1 with σ_{KS} and the phase coexistence equations

$$\Pi_i = \Pi_a \tag{13}$$

$$\mu_i = \mu_a \tag{14}$$

with Equations 10 and 11. Here the subscripts i and a represent the quantities associated with the isotropic and anisotropic phases, respectively.

The explicit expression for σ_{KS} is given only for $\alpha N \gg 1$ and $\alpha N \ll 1$ (Equation 8). Therefore the phase boundary concentrations c'_i and c'_a were calculated only for $N = 0$ (rod limit) and $N \geq 1.5$ as functions of N and the axial ratio $X[(L + d)/d]$, where c'_i and c'_a are the phase boundary number concentration between the isotropic and biphasic regions and that between the biphasic and liquid crystal regions, respectively. The numerical values of $v_0 c'_i$ and $v_0 c'_a$ are listed in Table I

TABLE I
(continued)

		N					
		0	1.5	2	3	4	5
$v_0 c'_a$	10	0.282	0.556	0.602	0.661	0.699	0.727
	20	0.171	0.419	0.470	0.540	0.587	0.621
	30	0.123	0.341	0.392	0.463	0.513	0.551
	40	0.0963	0.288	0.337	0.408	0.459	0.499
	50	0.0792	0.250	0.297	0.366	0.417	0.457
	60	0.0673	0.221	0.265	0.332	0.383	0.423
	80	0.0517	0.180	0.220	0.281	0.330	0.369
	100	0.0420	0.152	0.188	0.245	0.290	0.328
	200	0.0217	0.0858	0.109	0.149	0.183	0.214
	300	0.0146	0.0598	0.0768	0.107	0.135	0.159
	400	0.0110	0.0459	0.0594	0.0839	0.106	0.127
	500	0.0090	0.0373	0.0484	0.0689	0.0880	0.106

as functions of N and X . Figure 1 shows the calculated N dependence of the phase boundary concentrations at fixed axial ratio X . The values of $\nu_0 c'_i$ and $\nu_0 c'_a$ for N between 0 and 1.5 were obtained by the interpolation as shown by the solid curve in Figure 1.

Figure 2 shows the plots of the phase boundary concentrations vs. X at a constant persistence length $q = 37$ nm. Here the phase boundary concentrations are represented by the corresponding mass concentrations c_i and c_a . Solid curves were obtained from the extended scaled particle (ESP) theory and broken curves from the KS theory.¹³ It can be seen that the higher virial terms lower c_i and c_a and the effect is more enhanced for smaller q . The dash-dotted curves in Figure 2 represent the phase boundary concentrations calculated from the original SP theory (the Cotter theory¹²) for straight spherocylinders using the Onsager trial function for $f(\Omega)$. For large X , the deviation between the solid and dash-dotted curves is evident,

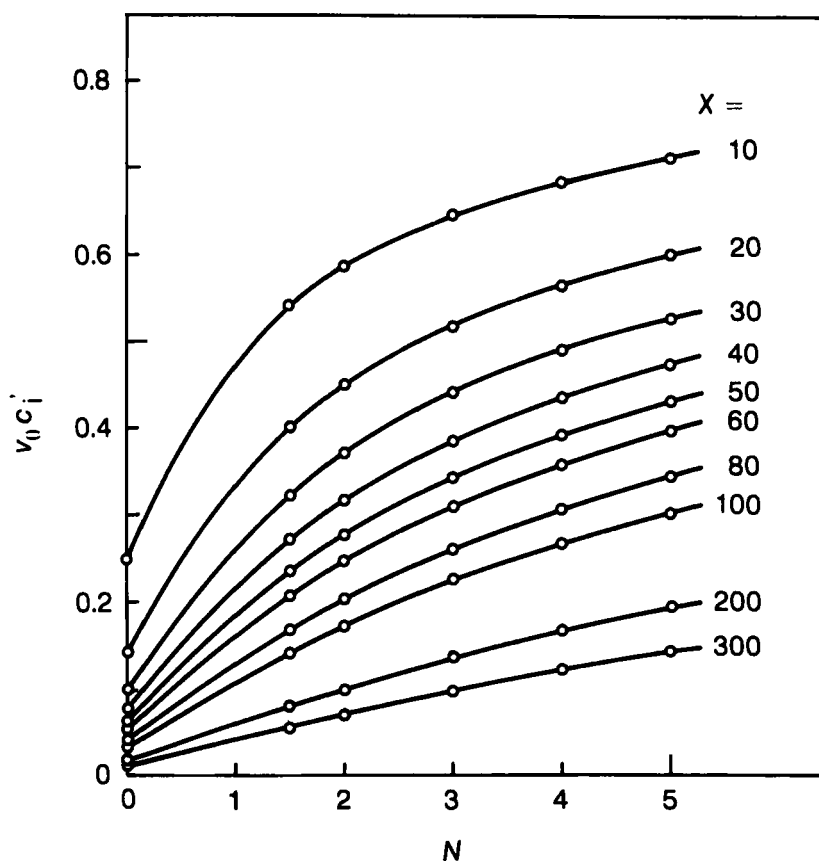


FIGURE 1 Isotropic-liquid crystal phase boundary concentrations for the wormlike spherocylinder solution calculated from the extended scaled particle (ESP) theory as a function of N at fixed axial ratios X . c'_i and c'_a , the phase boundary concentrations (number densities) between isotropic phase and biphasic regions and between liquid crystal phase and biphasic regions, respectively; ν_0 , the molecular volume of the spherocylinder.

demonstrating a remarkable effect of the chain flexibility on the phase boundary concentrations.

COMPARISON WITH EXPERIMENTAL DATA

In this section we compare the extended scaled particle (ESP) theory with experimental data of Π , c_i , and c_a for three systems: schizophyllan + water,^{8,9} PHIC + DCM, and PHIC + toluene.^{10,11} These experimental data are chosen for the comparison with theory, because they are for samples with narrow molecular weight distributions.²¹

In the calculation of Π , c_i , and c_a by the ESP theory, three molecular parameters must be given: the contour length L , the number of Kuhn's segment N , and the diameter d of each polymer. The values of L and N were calculated from the molecular weight of each sample using the molecular weight M_L per unit contour

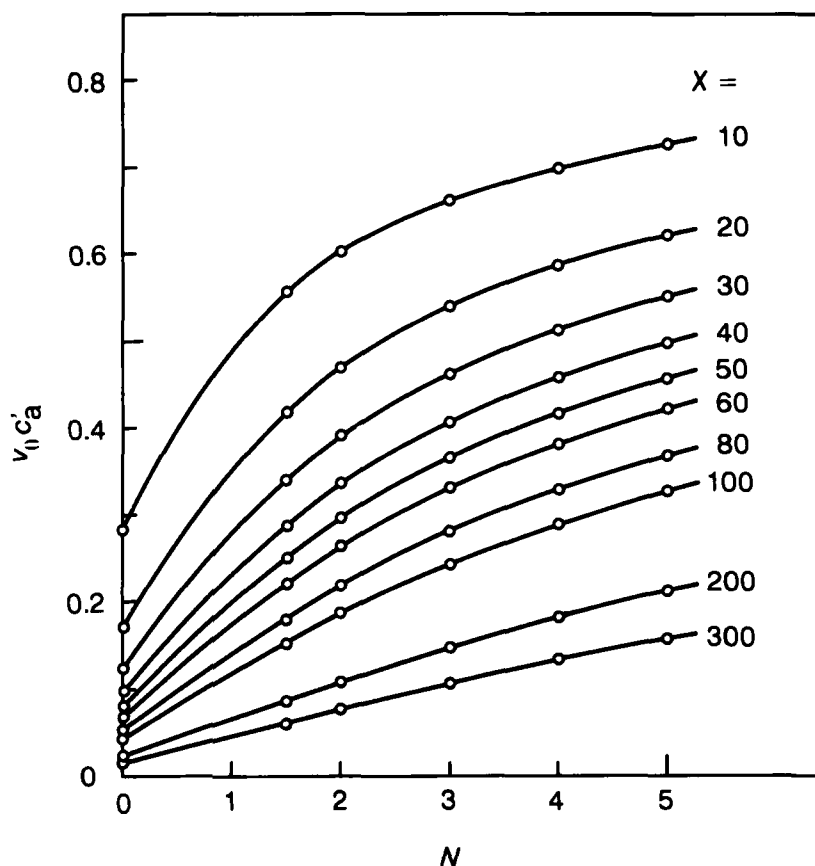


FIGURE 1 (continued)

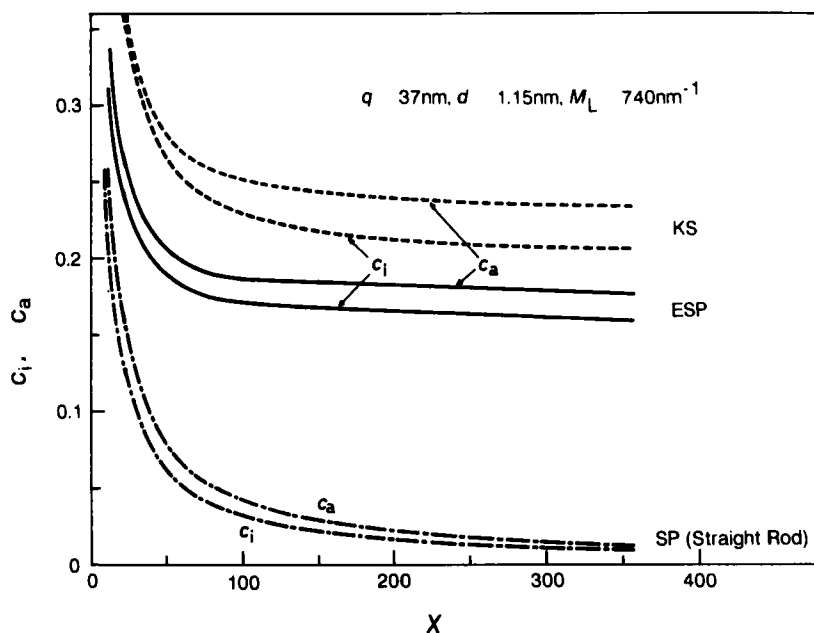


FIGURE 2 Theoretical phase boundary mass concentrations plotted against X for $d = 1.15$ nm; $q = 37$ nm; M_L (molecular weight per unit contour length) $= 740$ nm $^{-1}$. Solid curves, the ESP theory; dashed curves, the KS theory;¹³ dash-dotted curves, the original SP theory (the Cotter theory¹²) for straight spherocylinders.

length and the persistence length q : $M_L = 2150$ nm $^{-1}$ and $q = 200$ nm for schizophyllan in water;²² $M_L = 740$ nm $^{-1}$ and $q = 21$ nm for PHIC in DCM; $M_L = 740$ nm $^{-1}$ and $q = 37$ nm for PHIC in toluene.²¹ The value of the remaining parameter d was chosen so that the theoretical osmotic pressure best agreed with the experimental data. This same method had been used by Ogino and Kubo⁵ and Brian *et al.*⁷ in their data analyses. On the other hand, in the previous papers,^{10,11} the d value estimated from the partial specific volume of each polymer was used for comparing experimental data of Π , c_i , and c_a with the KS theory.

Figure 3a compares experimental data of Π for isotropic aqueous solutions of three schizophyllan samples with the theoretical values calculated from the ESP theory with $d = 1.52$ nm. (For the isotropic phase, Π in the ESP theory is the same as that in the original Cotter theory.) The ESP theory can reproduce the experimental concentration dependence of Π satisfactorily using $d = 1.52$ nm. The experimental phase boundary concentrations c_i and c_a are compared with the ESP theoretical values in Figure 3b, where circles and solid curves represent the experimental data and the ESP theoretical values for $d = 1.52$ nm, respectively. With the same d value as used in the calculation of Π , good agreement is obtained for c_i and c_a over the whole range of N studied. Experimental data for DCM and toluene solutions of PHIC are compared with the ESP theory in Figures 4 and 5, respectively. Again, reasonably good agreement between experiment and theory in Π , c_i , and c_a is obtained, when d is chosen to be 1.0 nm (DCM solutions) and

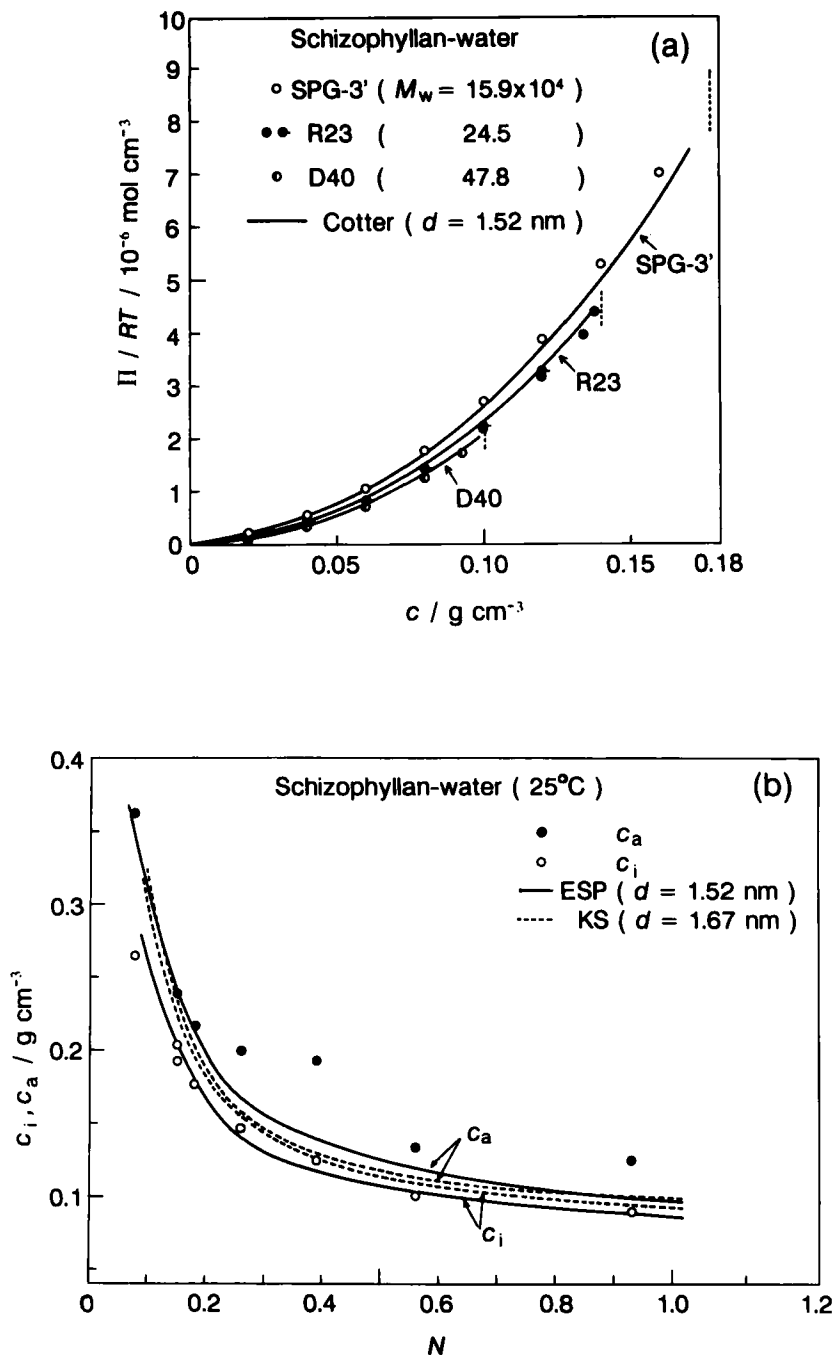


FIGURE 3 Comparison between theory and experiment for aqueous schizophyllan. (a) The polymer mass concentration c dependence of Π ; (b) N dependences of c_i and c_a . Circles, experimental data^{8,9}; solid curves, the ESP theory; broken curves, the KS theory¹³; vertical dotted lines in Panel a, experimental phase boundary concentrations c_i .

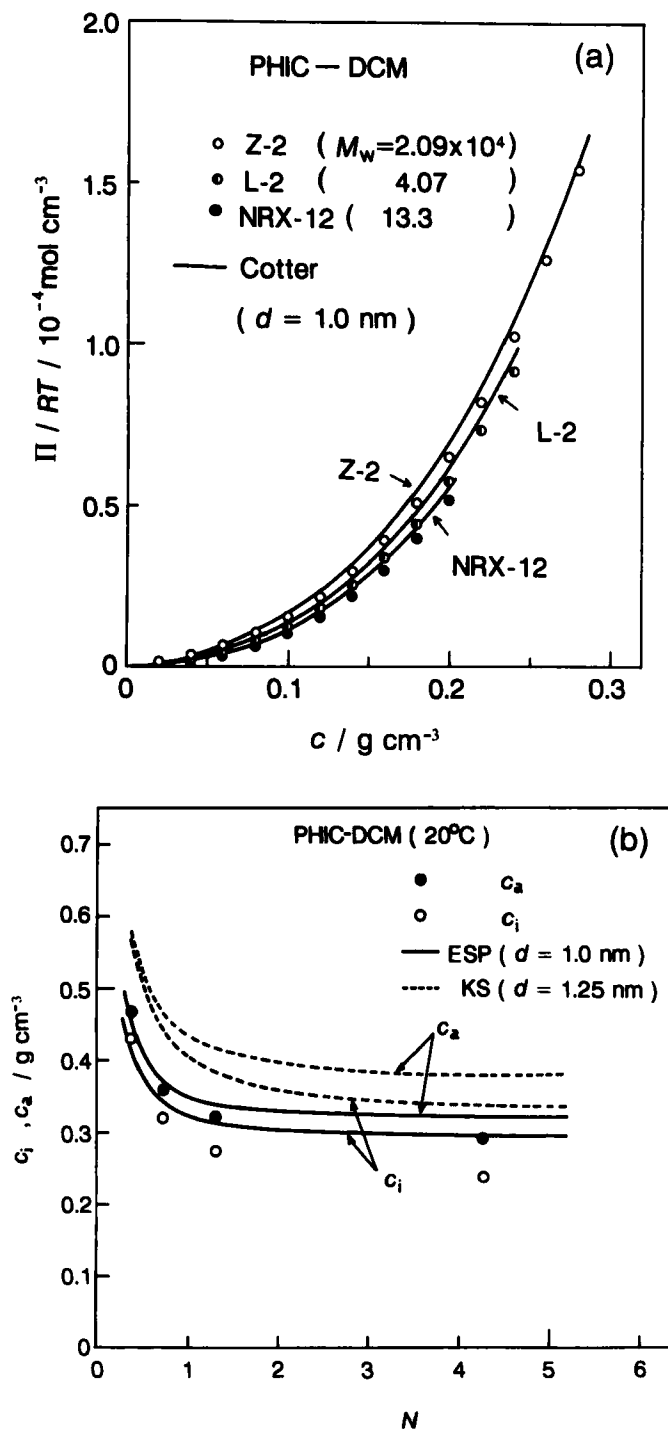


FIGURE 4 The same comparison as in Figure 3 for the system of PHIC and dichloromethane (DCM).^{10,11}

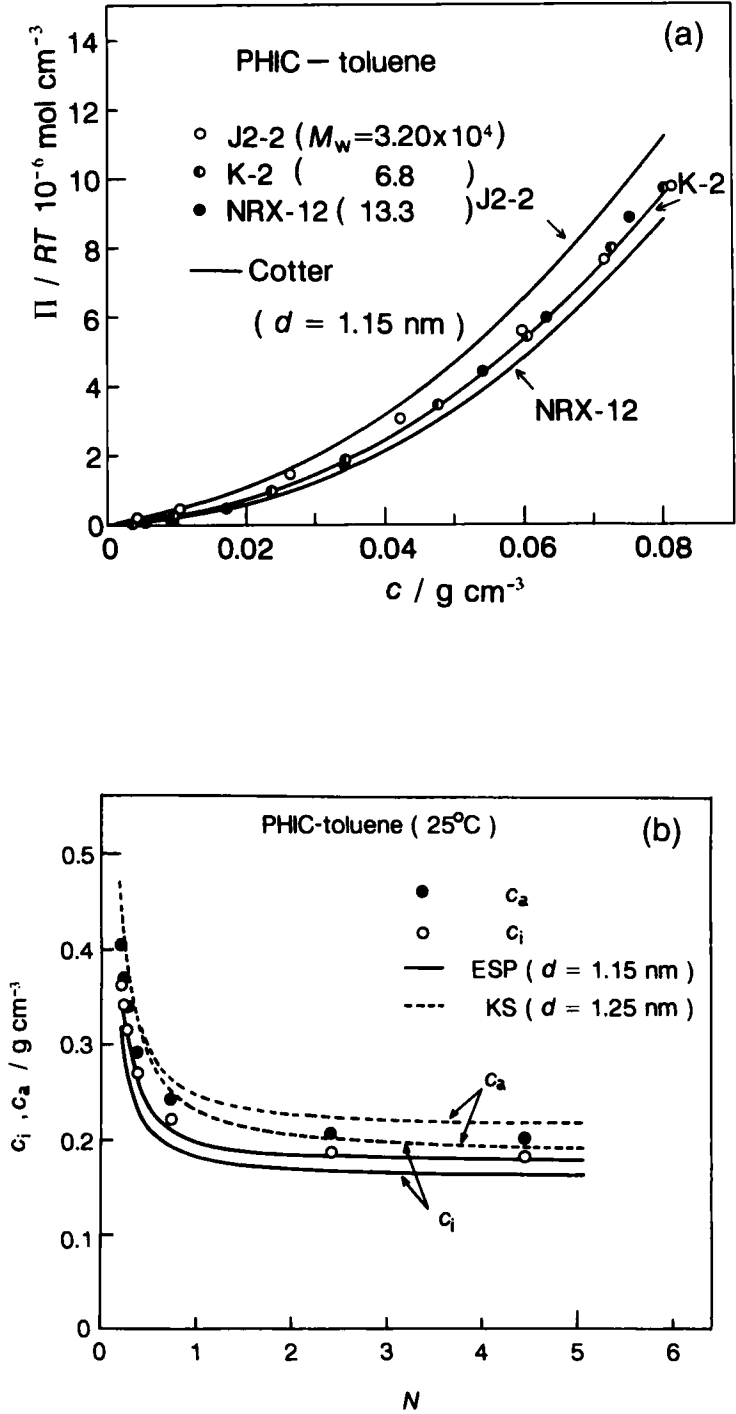


FIGURE 5 Same as for Figure 3 for the system of PHIC and toluene.^{10,11}

1.15 nm (toluene solutions). Thus, for all the three systems examined, the different kinds of thermodynamic quantities, Π and the phase boundary concentrations, can be explained consistently by the ESP theory.

The broken curves in Panels b of Figures 3–5 represent c_i and c_a calculated from the KS theory¹³ using d obtained from the partial specific volume of polymer. As mentioned in the previous paper,¹⁰ these curves for schizophyllan in water and PHIC in toluene are close to the experimental points, whereas those for PHIC in DCM appreciably deviate upward from the experimental data. PHIC in DCM is most flexible in the three cases, so that its phase boundary concentrations are highest. Therefore the effect of the third and higher virial terms in the free energy to the phase boundary concentrations may be most significant for this system. In fact, the solid curves of the ESP theory in Figure 4b are much closer to the experimental points than the broken curves, indicating that the disagreement of the KS theory in c_i and c_a of the PHIC-DCM system is mainly due to the higher virial terms neglected in the theory.

For all the three systems investigated, the value of d used in the ESP theory is rather close to that estimated from the partial specific volume of polymer (i.e., d used in the KS theory). This demonstrates that the isotropic-liquid crystal phase equilibrium in our systems can be explained essentially in terms of the hard-core potential.

APPENDIX

Equation 1 gives the third virial coefficient B_3 for spherocylinders as

$$B_3 = (b^2/3)[\rho(10X^{-1} + 8X^{-2}) + 29X^{-2} + 40X^{-3} + 40X^{-4}/3]$$

In the isotropic ($\rho = 1$) and the perfectly oriented ($\rho = 0$) states, this B_3 is rather close to Straley's B_3 ¹⁹ obtained from the numerical integration of the ternary cluster integral for hard long cylinders with $X = 10 - 50$:

$$\begin{aligned} B_3 &= 12.3(b^2/3)X^{-1} && \text{(isotropic state)} \\ &= 28.1(b^2/3)X^{-2} && \text{(perfectly oriented state)} \end{aligned}$$

However, in the imperfectly oriented state, Straley's B_3 was considerably larger than Cotter's for $30 \leq X \leq 50$. This difference may be due to the approximation employed in Straley's numerical calculation for the imperfect orientation. However a detailed comparison should be deferred until the numerical calculation is extended to a wider range of X .

References

1. W. Maier and A. Saupe, *Z. Naturforsch.*, **14a**, 882 (1959); **15a**, 287 (1960).
2. M. A. Cotter, *Mol. Cryst. Liq. Cryst.*, **97**, 29 (1983).

3. W. G. Miller, *Ann. Rev. Phys. Chem.*, **29**, 519 (1978).
4. P. J. Flory, *Adv. Polym. Sci.*, **59**, 1 (1984).
5. K. Kubo and K. Ogino, *Mol. Cryst. Liq. Cryst.*, **53**, 207 (1979).
6. K. Kubo, *Mol. Cryst. Liq. Cryst.*, **74**, 71 (1981).
7. A. A. Brian, H. L. Frisch, and L. S. Lerman, *Biopolymers*, **20**, 1305 (1981).
8. T. Itou, K. Van, and A. Teramoto, *J. Appl. Polym. Sci., Appl. Polym. Symp.*, **41**, 35 (1985).
9. K. Van and A. Teramoto, *Polym. J.*, **17**, 409 (1985).
10. T. Itou and A. Teramoto, *Macromolecules*, **21**, 2225 (1988).
11. T. Itou, T. Sato, A. Teramoto, and S. M. Aharoni, *Polym. J.*, **20**, 1049 (1988).
12. M. A. Cotter, *J. Chem. Phys.*, **66**, 1098 (1977).
13. (a) A. R. Khokhlov and A. N. Semenov, *Physica*, **108A**, 546 (1981); **112A**, 605 (1982); (b) T. Odijk, *Macromolecules*, **19**, 2313 (1986).
14. L. Onsager, *Ann. N. Y. Acad. Sci.*, **51**, 627 (1949).
15. H. Reiss, H. L. Frisch, and J. L. Lebowitz, *J. Chem. Phys.*, **31**, 369 (1959).
16. M. A. Cotter and D. E. Martire, *J. Chem. Phys.*, **53**, 4500 (1970).
17. G. Lasher, *J. Chem. Phys.*, **53**, 4141 (1970).
18. M. A. Cotter, *Phys. Rev. A*, **10**, 625 (1974).
19. J. P. Straley, *Mol. Cryst. Liq. Cryst.*, **24**, 7 (1973); also see Reference 13b.
20. H. Yamakawa and W. H. Stockmayer, *J. Chem. Phys.*, **57**, 2843 (1972).
21. There are same kinds of experimental data for PBLG solutions (e.g. Reference 5). However, these data were obtained using samples with a rather wide molecular weight distribution and then not used for the comparison with theory in this paper.
22. T. Yanaki, T. Norisuye, and H. Fujita, *Macromolecules*, **13**, 1462 (1980); Y. Kashiwagi, T. Norisuye, and H. Fujita, *Macromolecules*, **14**, 1220 (1981).
23. T. Itou, H. Chikiri, A. Teramoto, and S. M. Aharoni, *Polym. J.*, **20**, 143 (1988).